The Journal of Neuroscience, March 1995, 15(3): 2168–2178

Differential Modulation of α3β2 and α3β4 Neuronal Nicotinic Receptors Expressed in *Xenopus* Oocytes by Flufenamic Acid and Niflumic Acid

Ruud Zwart,[a] Marga Oortgiesen, and Henk P. M. Vijverberg

Research Institute of Toxicology, Utrecht University, NL-3508 TD Utrecht, The Netherlands

Effects of flufenamic acid (FFA) and niflumic acid (NFA), which are often used to block Ca^{2+}-activated Cl^- current, have been investigated in voltage-clamped *Xenopus* oocytes expressing α3β2 and α3β4 nicotinic ACh receptors (nAChRs). NFA and FFA inhibit α3β2 nAChR-mediated inward currents and potentiate α3β4 nAChR-mediated inward currents in normal, Cl^--free and Ca^{2+}-free solutions to a similar extent. The concentration-dependence of the inhibition of α3β2 nAChR-mediated ion current yields IC_{50} values of 90 μM for FFA and of 260 μM for NFA. The potentiation of α3β4 nAChR-mediated ion current by NFA yields an EC_{50} value of 30 μM, whereas the effect of FFA does not saturate for concentrations of up to 1 mM. At 100 μM, FFA reduces the maximum of the concentration–effect curve of ACh for α3β2 nAChRs, but leaves the EC_{50} of ACh unaffected. The same concentration of FFA potentiates α3β4 nAChR-mediated ion currents for all ACh concentrations and causes a small shift of the concentration–effect curve of ACh to lower agonist concentrations. The potentiation, like the inhibition, is most likely due to a noncompetitive effect of FFA. Increasing ACh-induced inward current either by raising the agonist concentration from 10 μM to 200 μM or by coapplication of 10 μM ACh and 200 μM FFA causes a similar enhancement of block of the α3β4 nAChR-mediated ion current by Mg^{2+}. This suggests that the effects of FFA and of an increased agonist concentration result in a similar functional modification of the α3β4 nAChR-operated ion channel. It is concluded that α3β4 and α3β2 nAChRs are oppositely modulated by FFA and NFA through a direct β-subunit-dependent effect.

[Key words: neuronal nicotinic ACh receptors,* Xenopus *oocytes, inhibition, potentiation, chloride channel blockers, flufenamic acid, niflumic acid, voltage clamp]

Received Jan. 21, 1994; revised Sept. 12, 1994; accepted Sept. 15, 1994.

We thank Dr. Jim Patrick (Baylor College of Medicine, Houston, Texas) for providing research facilities, Marietta Piattoni (Baylor College of Medicine), Sjeng Horbach (Research Institute of Toxiciology, Utrecht), and Jenny Narraway (Hubrecht Laboratory, Utrecht) for plasmid propagation and oocyte preparation, and Aart de Groot (Research Institute of Toxicology) for computer support. This work was financially supported by Shell Internationale Research Maatschappij B.V. and by a travel grant from the Netherlands Organization for Scientific Research (N.W.O.).

Correspondence should be addressed to Dr. H. Vijverberg, Research Institute of Toxicology, Utrecht University, P.O. Box 80.176, NL-3508 TD Utrecht, The Netherlands.

[a]Present address: Max Planck Institute for Experimental Medicine, Department of Molecular Neuroendocrinology, Hermann-Rein-Strasse 3, D-37075 Göttingen, Germany.

Neuronal nicotinic acetylcholine receptors (nAChRs) belong to the family of ligand-gated ion channels and are found throughout the CNS and PNS (Luetje et al., 1990). Molecular cloning studies have provided evidence for the existence of at least six different types of α-subunits of mammalian neuronal nAChRs, named α2-α7 (Wada et al., 1988; Boulter et al., 1986, 1990; Goldman et al., 1987; Lamar et al. 1990; Séguéla et al., 1993) and three different types of β-subunits, β2-β4 (Deneris et al., 1988a,b; Duvoisin et al., 1989). Oocyte expression studies have demonstrated that each of the α2, α3, and α4 subunits may be combined with β2 or β4 to obtain functional hetero-oligomeric nAChRs (Boulter et al., 1987; Deneris et al., 1988; Wada et al., 1988; Duvoisin et al., 1989; Luetje and Patrick, 1991). The α7 subunit forms homo-oligomeric channels in oocytes (Couturier et al., 1990; Schoepfer et al., 1990; Séguéla et al., 1993) and the functional significance of α5, α6, and β3 is presently unknown (Deneris et al., 1991). By analogy to the pentameric endplate nicotinic receptor, the hetero-oligomeric neuronal nAChRs are supposed to contain two α- and three β-subunits (Anand et al., 1991; Cooper et al., 1991).

The expression of different combinations of subunits in *Xenopus* oocytes results in neuronal nAChRs with distinct pharmacological and physiological properties. The features of α3β2 and α3β4 subunit combinations have been investigated to some detail. As compared to the α3β2 nAChR, the α3β4 nAChR is more sensitive to the agonists ACh and cytisine (Cachelin and Jaggi, 1991; Luetje and Patrick, 1991), is much less sensitive to block by the antagonist neuronal bungarotoxin (Duvoisin et al., 1989; but see Papke et al., 1993) and by substance P (Stafford et al., 1994), desensitizes much more slowly (Cachelin and Jaggi, 1991), and exhibits prolonged single channel bursting and a higher single channel conductance (Papke and Heinemann, 1991).

In various types of mammalian cells the ion channels of native neuronal nAChRs appear permeable to Ca^{2+} (Fieber and Adams, 1991; Sands and Barish, 1991; Mulle et al., 1992a; Vernino et al., 1992; Trouslard et al., 1993; Zhou and Neher, 1993). However, multiple types of nAChR may be expressed in the same cell (Vernallis et al., 1993) and the subunit composition of native nAChRs is unknown. In oocytes it has been demonstrated that the homo-oligomeric α7 nAChR is much more permeable to Ca^{2+} than to Na^+ (Galzi et al., 1992; Bertrand et al., 1993; Séguéla et al., 1993). Although the relative Ca^{2+} permeabilities of defined hetero-oligomeric nAChRs remains to be established, they may carry sufficient Ca^{2+} current (Vernino et al., 1992) to activate an endogenous Ca^{2+}-dependent Cl^- [Cl(Ca)] current in oocytes (Barish, 1983). Apart from permeating through the ion

channel, external divalent cations allosterically modulate neuronal nAChR function. Increasing the external Ca^{2+} concentration causes a simultaneous reduction of the single channel conductance and increase of the channel opening frequency, resulting in a net enhancement of the amplitude of the whole-cell ACh response (Fieber and Adams, 1991; Mulle et al., 1992b; Vernino et al., 1992). A similar effect of external Mg^{2+} on single channel conductance has been reported, but Mg^{2+} hardly affects the whole-cell ACh response (Mulle et al., 1992b).

In order to investigate Ca^{2+} permeable channels in *Xenopus* oocytes, the endogenous Cl(Ca) current is routinely suppressed by high concentrations of flufenamic acid (FFA; IC_{50} = 28 μM) and niflumic acid (NFA; IC_{50} = 17 μM) (Leonard and Kelso, 1990; White and Aylwin, 1990; Vernino et al., 1992; Séguéla et al., 1993). Alternatively, the endogenous Cl(Ca) current can be eliminated by replacement of external Ca^{2+} by Mg^{2+}, Sr^{2+}, or Ba^{2+} and by chelation of intracellular Ca^{2+} (Barish, 1983; Miledi and Parker, 1984; Galzi et al., 1992; Sands et al., 1993). In addition, methanesulfonate does not permeate through the Cl(Ca) channel in *Xenopus* oocytes (Barish, 1983).

As fenamates have also been shown to act as noncompetitive antagonists of NMDA receptors in primary cultured rat spinal neurons (Lerma and Martín del Río, 1992) and of rat cerebral cortex $GABA_A$ receptors expressed in *Xenopus* oocytes (Woodward et al., 1994), we have investigated potential effects of FFA and NFA on nAChRs. The results indicate that the chloride channel blockers cause direct and opposite effects on α3β2 and α3β4 nAChRs.

Materials and Methods

Materials. Mature female specimens of *Xenopus laevis* were obtained from Nasco (Fort Atkinson, WI). Acetylcholine chloride, atropine sulfate, 3-aminobenzoic acid ethyl ester, collagenase type I, flufenamic acid, and niflumic acid (Fig. 1) were purchased from Sigma (St. Louis, MO) and methanesulfonate from Aldrich (Milwaukee, WI).

Expression in Xenopus *oocytes.* Frogs were anesthetized by submersion in 0.1% 3-aminobenzoic acid ethyl ester. Oocytes were surgically removed and defolliculated after treatment with 1.5 mg/ml collagenase type I in Ca^{2+}-free modified Barth's saline for 2 hr at room temperature. cDNAs for α3, β2, and β4 were ligated into the pSM plasmid vector containing the SV40 viral promotor. The α3 construct and either one of the two β-constructs were coinjected at a molar ratio of 1:1 into the nuclei of stage V and VI oocytes within 24 hr after harvesting using a Drummond microinjector (Bertrand et al., 1991). Subunits were dissolved in distilled water and the total injection volume was about 20 nl per oocyte, corresponding to 7–10 ng DNA of each subunit. Injected oocytes were incubated at 19°C for 2–5 d in Cl^--containing or Cl^--free modified Barth's saline, to be investigated under Cl^- or Cl^--free conditions, respectively.

Solutions. Modified Barth's saline contained (in mM) 88 NaCl, 1 KCl, 2.4 $NaHCO_3$, 0.3 $Ca(NO_3)_2$, 0.41 $CaCl_2$, 0.82 $MgSO_4$, 15 HEPES, and 100 μg/ml gentamicin (pH = 7.6 with NaOH). Cl^--free modified Barth's saline contained (in mM) 90 NaOH, 2.5 KOH, 10 HEPES, 2 $Ca(OH)_2$, 0.8 $Mg(OH)_2$, and 100 μg/ml gentamicin (pH = 7.6 with methanesulfonate). During voltage clamp oocytes were superfused with Cl^- saline containing (in mM) 115 NaCl, 2.5 KCl, 1 $CaCl_2$, 10 HEPES (pH = 7.2 with NaOH) or with Cl^--free saline containing (in mM) 115 NaOH, 2.5 KOH, 1 $Ca(OH)_2$, 10 HEPES (pH = 7.2 with methanesulfonate). All superfusates contained 1 μM atropine to block endogenous muscarinic responses.

Electrophysiology. Oocytes were voltage clamped by the standard two microelectrode voltage-clamp technique using an Axoclamp 2A voltage-clamp amplifier (Axon Instruments, Burlingame, CA). Microelectrodes (0.5–2.5 MΩ) were filled with 3 M KCl under standard conditions or with 3 M K-methanesulfonate and 50 mM KCl under Cl^--free conditions. The holding potential was −60 mV, unless otherwise indicated. All experiments were performed at room temperature (20–23°C).

Voltage clamped oocytes were continuously superfused with saline solution at a rate of approximately 20 ml/min. Aliquots of stock solutions of 0.1–1 M of niflumic acid and flufenamic acid in dimethylsulfoxide (DMSO) and of ACh in distilled water were added to the saline immediately before the experiments. Drugs were applied by switching between control and drug-containing saline using a solenoid valve. Agonist applications were alternated with 5 min of superfusion with agonist-free saline to allow the receptors to recover completely from desensitization. Final DMSO concentrations never exceeded 0.2% (v/v), which had no effect on α3β2 and α3β4 nAChR-mediated inward currents in control experiments.

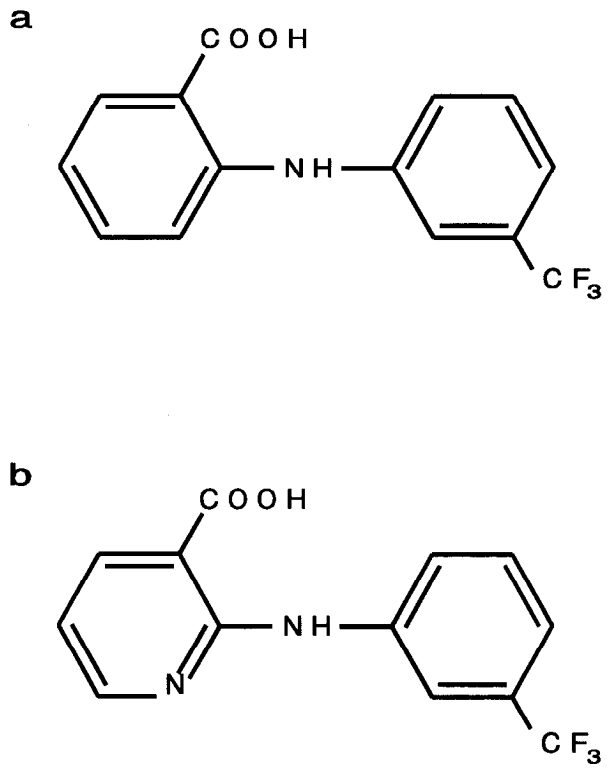

Figure 1. Structural formulas of flufenamic acid (*a*) and of niflumic acid (*b*).

Currents were low-pass filtered (eight-pole Bessel, Frequency Devices, Haverhill, MA) at 150 Hz unless otherwise indicated, digitized and stored by a Macintosh IIci computer using data acquisition software (LABVIEW, National Instruments, Austin, TX and LIB I, University of Arizona, Tucson, AZ).

Concentration–effect curves were fitted by a nonlinear least-squares algorithm (Marquardt, 1963) according to the equation $i = i_{max}/(1 + \{EC_{50}/[conc]\}^n)$, where n and EC_{50} represent the slope factor and the agonist concentration producing half-maximal response, respectively. Results are expressed as mean ± SD of n independent experiments.

Results

Direct effects of flufenamic acid and niflumic acid on neuronal nAChR-mediated ion current

Under standard Cl^- conditions the superfusion of oocytes with 100 μM and 10 μM ACh, that is, nearly equipotent concentrations for α3β2 and α3β4 nAChRs, respectively (Cachelin and Jaggi, 1991), evoked the typical desensitizing and nondesensitizing inward currents (Fig. 2). After 15 min of superfusion with a mixture of 100 μM FFA and 100 μM NFA, which is commonly used to suppress endogenous Cl(Ca) current in *Xenopus* oocytes (Vernino et al., 1992; Séguéla et al., 1993), the peak amplitude of the α3β2 nAChR-mediated inward currents was steadily reduced to 23 ± 3% (n = 3) of control values (Fig. 2*a*). Conversely, after 15 min of superfusion with the same mixture, the peak amplitude of α3β4 nAChR-mediated inward currents was potentiated to 197 ± 25% (n = 5) of control values (Fig. 2*b*).

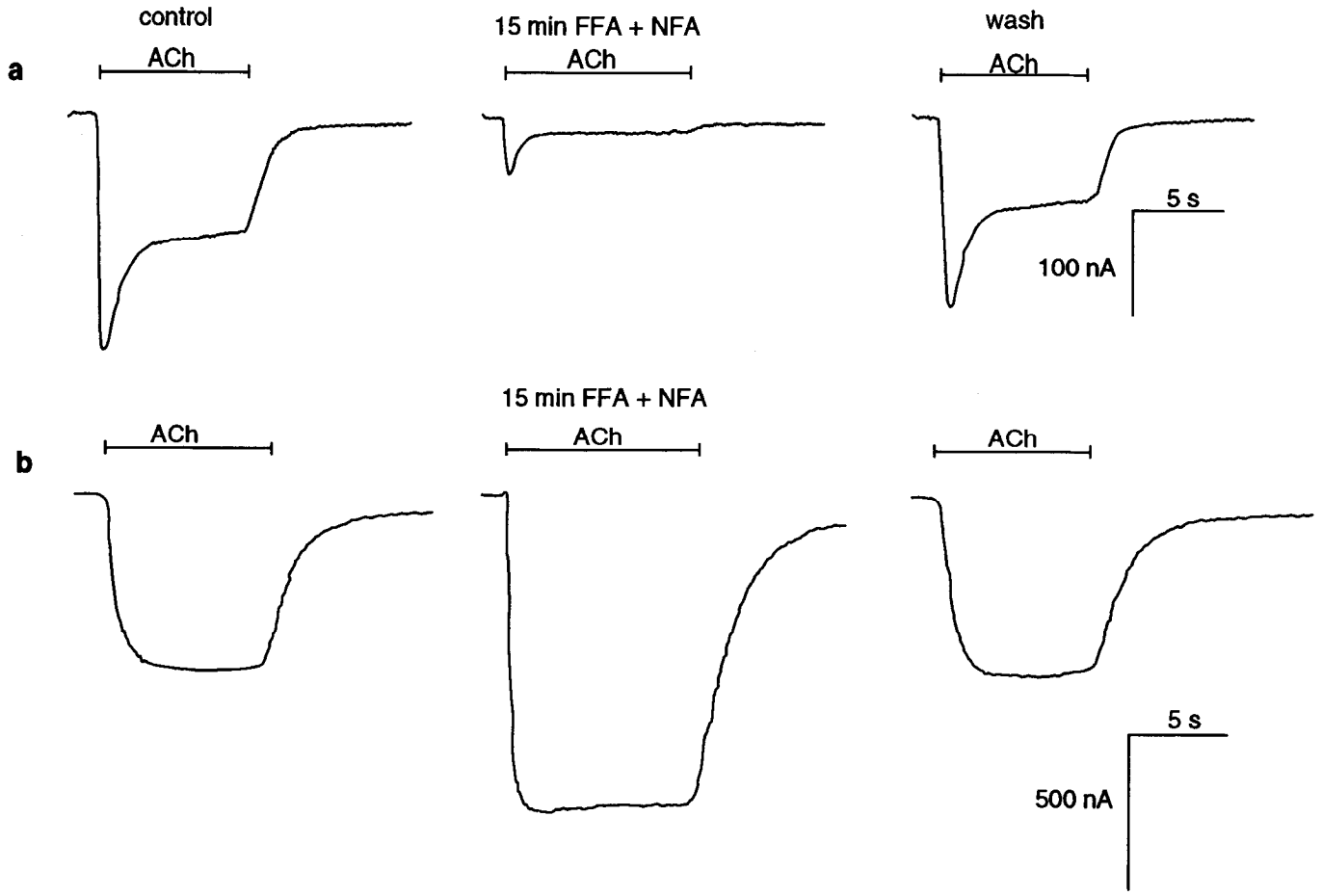

Figure 2. Differential effects of FFA and NFA on α3β2 and α3β4 nAChRs. A mixture of 100 μM NFA and 100 μM FFA inhibits α3β2 nAChR-(*a*) and potentiates α3β4 nAChR-mediated inward currents (*b*) recorded in Cl^- saline. Inward currents were evoked by superfusion of 100 μM ACh (*a*) and 10 μM ACh (*b*) as indicated by *horizontal bars*. After 15 min of superfusion with NFA and FFA, the peak amplitude of the α3β2 nAChR-mediated inward current was reduced to 25% of the control value, whereas the peak amplitude of the α3β4 nAChR-mediated inward current was increased to 176% of the control value. Both effects were reversed after the removal of NFA and FFA by washing with Cl^- saline.

The inhibitory and potentiating effects were both reversed on washing with Cl^- saline (Fig. 2*a*,*b*).

The effects of the Cl(Ca) current blockers were further investigated in oocytes incubated in Cl^--free modified Barth's solution and voltage clamped in Cl^--free saline. In the experiments of Figure 3, Ca^{2+} was replaced by 1 mM Mg^{2+} or 1 mM Ba^{2+}, which are ineffective in activating Cl(Ca) current in oocytes (Barish, 1983; Miledi and Parker, 1984). These experimental conditions are most unfavorable for the activation of Cl(Ca) current. Even under these conditions the mixture of 100 μM FFA and 100 μM NFA reduced the peak amplitude of α3β2 nAChR-mediated ion currents to 22 ± 5% (n = 3) of the control values (Fig. 3*a*) and increased that of the α3β4 nAChR-mediated ion current to 169 ± 24% (n = 3) of control values (Fig. 3*b*). These effects are qualitatively the same as and cannot be distinguished from those obtained under standard conditions within experimental error (Student's t test, p = 0.78 and 0.17, respectively).

Figure 4 shows the effects of coapplication of ACh with the mixture of 100 μM FFA and 100 μM NFA on α3β2 and α3β4 nAChR-mediated inward currents. The effect of the mixture on the α3β2 nAChR was incomplete on coapplication with ACh (Fig. 4*a*). Steady-state inhibition was not reached until 5–10 min of superfusion of the oocytes with NFA and FFA (not shown). Conversely, the potentiation of α3β4 nAChR-mediated ion currents by the mixture of FFA and NFA appeared already complete on the first coapplication and amounted to 187 ± 15% (n = 4). This effect is the same as that observed after 15 min of superfusion with FFA and NFA under standard Cl^- conditions and under Ca^{2+}-free and Cl^--free conditions. When applied alone, neither the mixture of FFA and NFA nor the individual compounds caused detectable changes in membrane current (not shown).

Concentration-dependent effects of FFA and of NFA

In order to investigate the concentration-dependent effects of FFA and of NFA on α3β2 and α3β4 nAChRs, oocytes were superfused with various concentrations of the individual compounds under Cl^--free conditions. The peak amplitude of α3β2 nAChR-mediated inward currents was reduced after 10 min of superfusion of FFA (Fig. 5*a*) and NFA (Fig. 5*b*) in a concentration-dependent manner. In addition, the decay of 100 μM ACh-induced inward currents became faster with increasing concentrations of FFA and NFA, and the amplitude of the steady inward current component was reduced by FFA and NFA. The concentration–effect curves for the reduction of peak amplitudes of the α3β2 nAChR-mediated inward currents by FFA and NFA are shown in Figure 5*c*. The fitted concentration–effect curves yielded estimates for the IC_{50} and slope factor of 90 ± 4 μM and

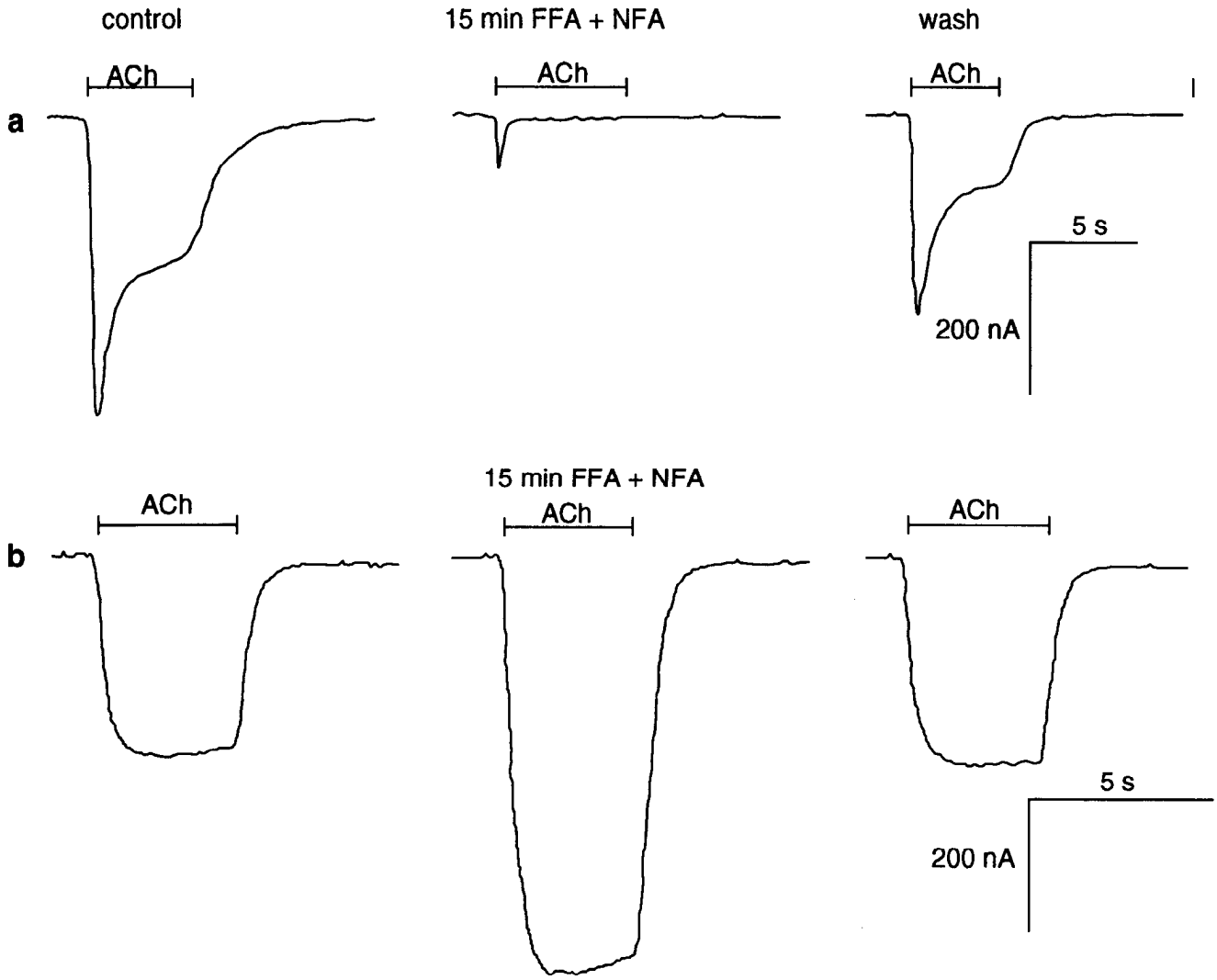

Figure 3. Effects of FFA and NFA on α3β2 and α3β4 nAChRs under Ca^{2+}-free and Cl^--free conditions. The mixture of 100 μM NFA and 100 μM FFA inhibits α3β2 nAChR- (*a*) and potentiates α3β4 nAChR-mediated inward currents (*b*) recorded under Ca^{2+}-free and Cl^--free conditions. Inward currents were evoked by superfusion of 100 μM (*a*) and 10 μM ACh (*b*) as indicated by *horizontal bars*. After 15 min of superfusion of NFA and FFA, the peak amplitude of the α3β2 nAChR-mediated inward current was reduced to 15% of the control value, whereas the peak amplitude of the α3β4 nAChR-mediated inward current was increased to 206% of the control value. The effects were reversed after the removal of NFA and FFA by washing with Ca^{2+}-free and Cl^--free saline.

-1.3 ± 0.1 for FFA, and 260 ± 30 μM and -1.5 ± 0.2 for NFA.

The potentiating effects of FFA and NFA on α3β4 nAChR-mediated inward currents are shown in Figure 6. Peak amplitudes of inward currents were increased on coapplication of 10 μM ACh with FFA (Fig. 6*a*) and NFA (Fig. 6*b*) in a concentration-dependent manner. Control experiments showed that the potentiating effect of 1 μM FFA also reached steady-state on coapplication with ACh. The concentration–effect curve fitted to the data obtained with NFA (Fig. 6*c*) yielded an EC_{50} value of 30 ± 13 μM, a slope factor of 0.88 ± 0.22 and a maximum response amplitude of $159 \pm 4\%$ relative to control. The data in Figure 6*c* show that the potentiating effect of FFA did not saturate up to the highest concentration used, which was at the solubility limit. Therefore, a concentration–effect curve could not be fitted for FFA. At concentrations of 1 mM, FFA and NFA potentiated the α3β4 nAChR-mediated inward currents, evoked by superfusion of 10 μM ACh, to $328 \pm 10\%$ ($n = 3$) and $156 \pm 12\%$ ($n = 4$) of control values, respectively.

Effects of FFA on the concentration–effect curves of ACh

The inhibitory and potentiating effects of FFA on α3β2 and α3β4 nAChRs have been studied in more detail. Inward currents mediated by α3β2 nAChRs evoked by various concentrations of ACh in the absence and presence of 100 μM FFA in Ca^{2+}-free Cl^- saline containing 1 mM Ba^{2+} are shown in Figure 7*a*. The dependence of the peak inward current amplitude on ACh concentration under control conditions and in the presence of 100 μM FFA is shown in Figure 7*b*. The results show that FFA causes a reduction of the peak amplitudes of α3β2 nAChR-mediated inward currents at all ACh concentrations. The mean of the EC_{50} values and slope factors of concentration–effect curves fitted to the data obtained from three oocytes were 30 ± 14 μM ACh and 0.85 ± 0.18 in control experiments, and $41 \pm$

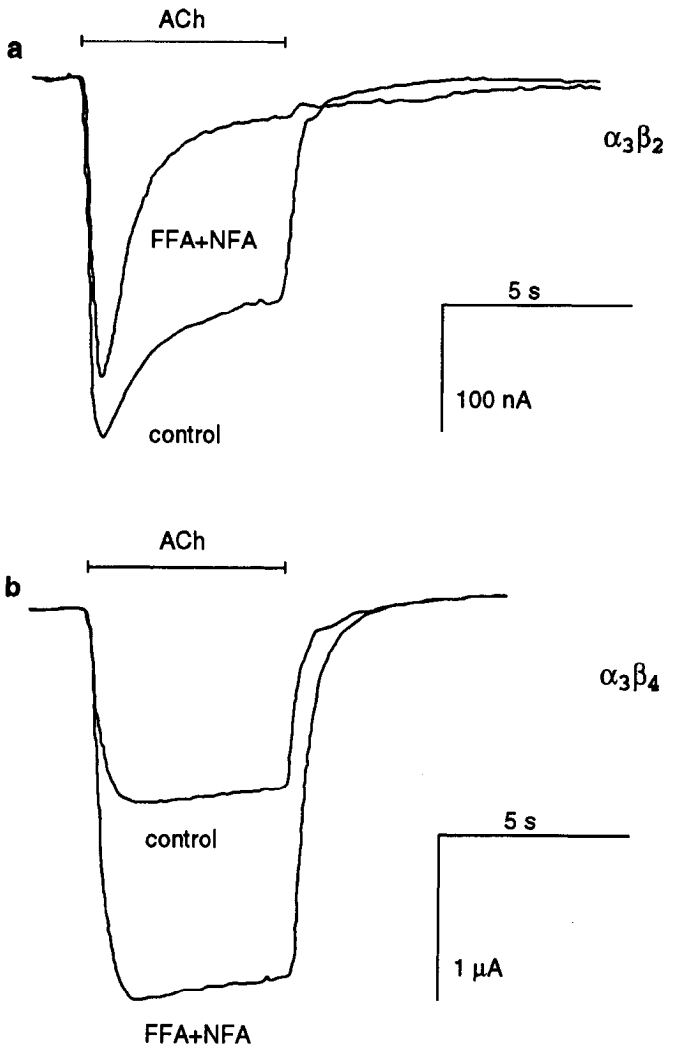

Figure 4. Onset of inhibitory and potentiating effects. Effects of coapplication of 100 μM NFA and 100 μM FFA with 100 μM ACh on α3β2 (*a*) and with 10 μM ACh on α3β4 nAChR-mediated inward current (*b*). The coapplications show only the onset of the inhibitory effect on α3β2 nAChR-mediated inward current, whereas the potentiating effect on α3β4 nAChR-mediated inward current cannot be distinguished from the steady-state effect.

30 μM ACh and 0.73 ± 0.23 in the presence of 100 μM FFA. On average the maximum of the concentration–effect curve of ACh was reduced by 100 μM FFA to 38 ± 8% of the control value (Fig. 7*b*). The changes of the EC_{50} value and slope factor observed induced by FFA are not significant within experimental error, whereas the maximum inward current amplitude is decreased significantly (Student's *t* test, $p < 0.001$).

Inward currents mediated by α3β4 nAChRs evoked by various concentrations of ACh in the absence and presence of 100 μM FFA in Cl^--free saline are shown in Figure 8*a*. The dependence of the peak inward current amplitude on ACh concentration under control conditions and in the presence of 100 μM FFA is shown in Figure 8*b*. The results show that in the presence of 100 μM FFA the amplitudes of α3β4 nAChR-mediated inward currents are enhanced at all agonist concentrations and that tail currents on the removal of high concentrations of the agonist are also enhanced by FFA. Fitting concentration–effect curves to the data obtained from four oocytes yielded mean EC_{50} values and slope factors of 63 ± 23 μM ACh and 1.47 ± 0.16 in the control situation, and of 37 ± 14 μM ACh and 1.48 ± 0.35 in the presence of 100 μM FFA. On average 100 μM FFA enhances the maximum of the concentration–effect curve of ACh to 118 ± 9% of the control value (Fig. 8*b*). The changes of the EC_{50} value and slope factor observed induced by FFA are not significant within experimental error, whereas the maximum inward current amplitude is enhanced significantly (Student's *t* test, $p < 0.001$).

Relation between FFA effect on α3β4 nAChR and divalent cation concentration

Since FFA and divalent cations both modulate the responses mediated by neuronal type nAChRs the interaction between the two was also investigated. Experiments were performed under Cl^--free conditions and the concentration of Mg^{2+} was varied in order to maintain a low probability of Cl(Ca) channel activation. In control experiments α3β4 nAChR-mediated ion currents were evoked by coapplications of 10 μM ACh and 1–30 mM Mg^{2+}. A slight, but significant potentiation was observed with increasing Mg^{2+} concentration (Fig. 9*a*), whereas concentration-dependent block was observed in the continuous presence of 200 μM FFA (Fig. 9*b*). A similar concentration-dependent block by Mg^{2+} was observed when responses were evoked by 200 μM ACh instead of 10 μM ACh (Fig. 9*c*).

Discussion

Direct effects of niflumic acid and flufenamic acid on neuronal nAChRs

In this article we demonstrate that the compounds NFA and FFA, which are commonly used to block endogenous Cl(Ca) current in *Xenopus* oocytes, differentially affect α3β4 and α3β2 neuronal nAChRs. Surprisingly, α3β4 nAChR-mediated inward currents are potentiated by these compounds, whereas the α3β2 nAChR-mediated inward currents are reduced.

The effects of NFA and FFA appear to originate from a direct interaction with the nAChRs for a number of reasons. The potentiation of α3β4 nAChR-mediated inward currents under standard Cl^- conditions (Fig. 2) cannot be explained by Cl(Ca) current block. Cl(Ca) current block at the holding potential of −60 mV should have resulted in a reduction of the amplitude of the ACh-induced inward current, since the Cl^- current reversal potential in oocytes is about −25 mV (Barish, 1983). In addition, the differential effects on α3β4 and α3β2 nAChRs cannot be accounted for at the same time by block of Cl(Ca) current and were also observed at potentials near the reversal potential for Cl^- (not shown). Potentiation and inhibition were similar under standard Cl^- conditions (Fig. 2), Cl^--free conditions (Figs. 5, 6) and even when external Ca^{2+} was replaced by Mg^{2+} or Ba^{2+} under Cl^--free conditions (Fig. 3). The complete block of α3β2 nAChR-mediated currents by high concentrations of NFA and

→

Figure 5. Concentration-dependent effects of FFA and NFA on α3β2 nAChRs. *a, Left column* shows control, 100 μM ACh-induced inward currents and the *right column* shows the 100 μM ACh-induced inward currents in the same oocytes after 10 min of superfusion with FFA at concentrations of 30, 300, and 1000 μM as indicated. *b, Left column* shows control, 100 μM ACh-induced inward currents and the *right column*

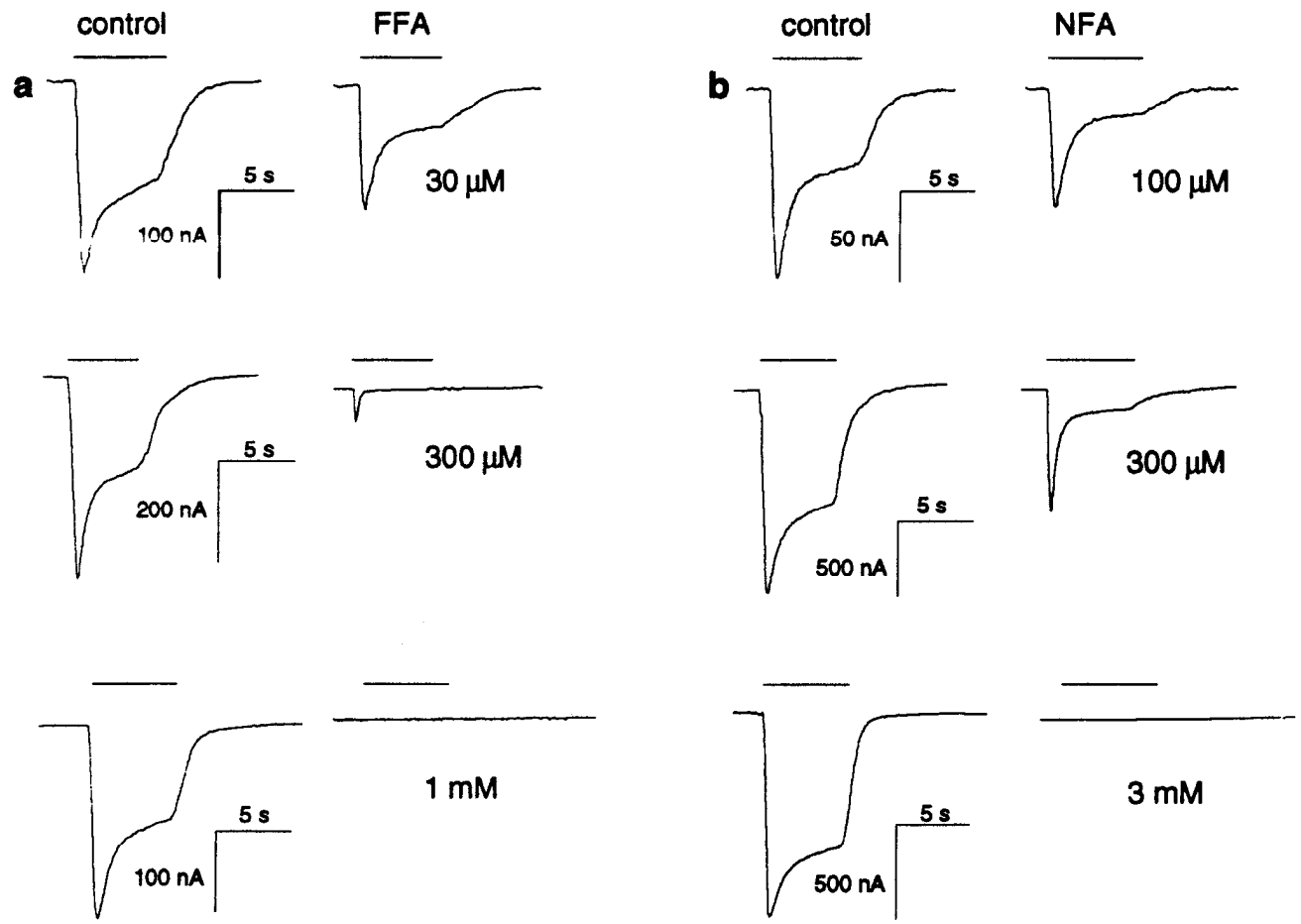

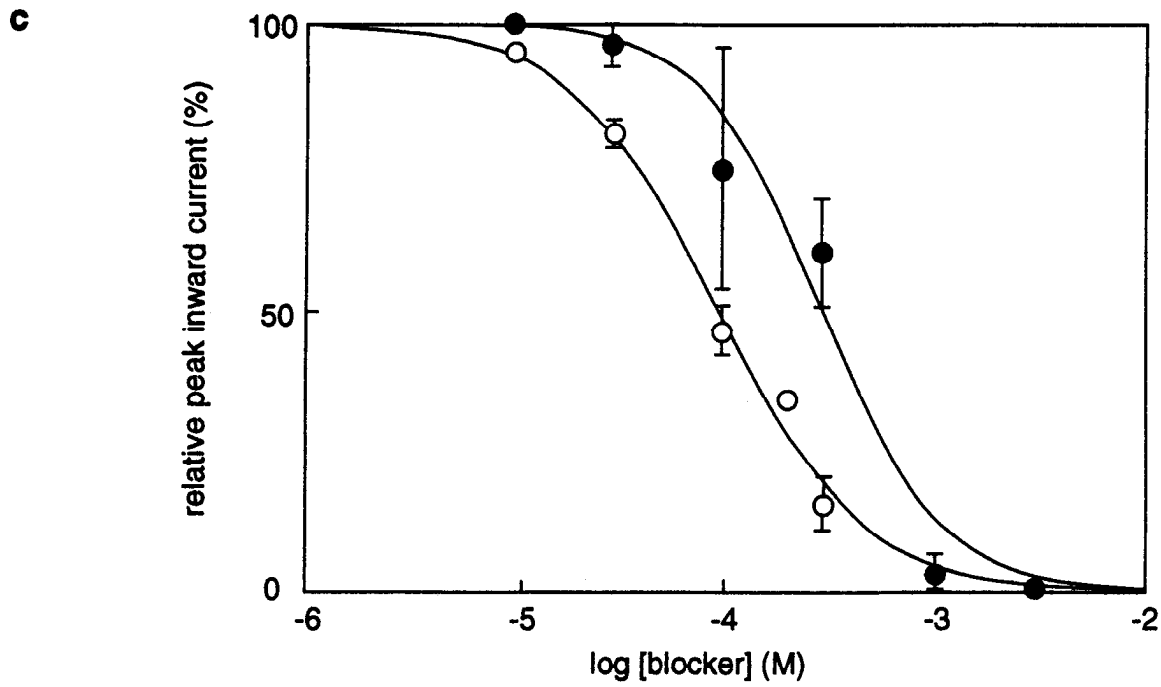

shows the 100 μM ACh-induced inward currents in the same oocytes after 10 min of superfusion with NFA at concentrations of 100, 300, and 3000 μM as indicated. *c*, Concentration–effect curves of FFA (*open circles*) and NFA (*solid circles*) for the reduction of the peak amplitude of 100 μM ACh-induced inward current mediated by α3β2 nAChRs. Data points represent mean ± SD (error bars) of three to five oocytes.

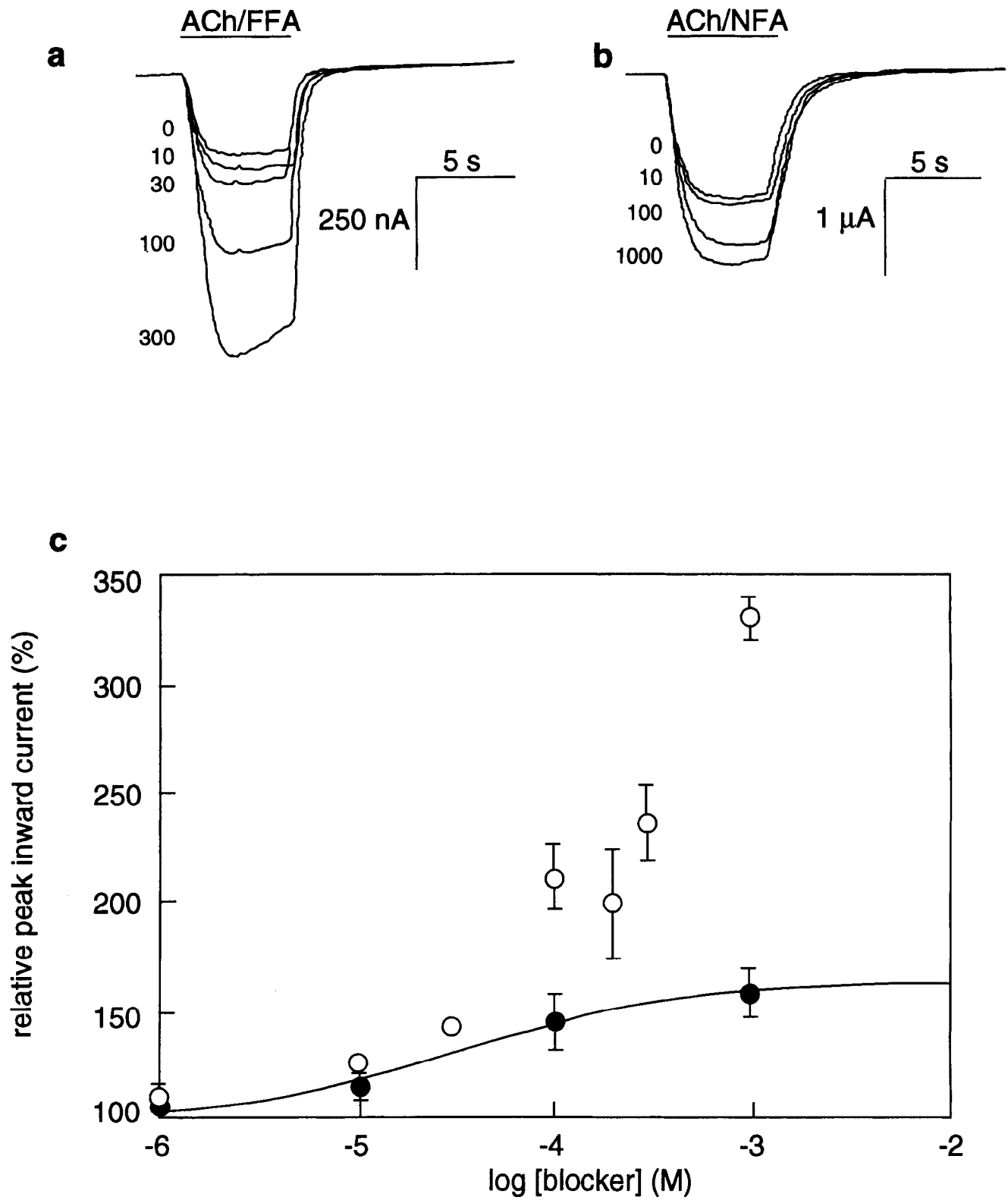

Figure 6. Concentration-dependent effects of FFA and NFA on α3β4 nAChRs. *a*, Control, 10 μM ACh-induced inward current and superimposed inward currents recorded from the same oocyte during coapplication of 10 μM ACh and FFA at concentrations of 10, 30, 100, and 300 μM as indicated. *b*, Control, 10 μM ACh-induced inward current and superimposed inward currents recorded from the same oocyte during coapplication of 10 μM ACh and NFA at concentrations of 10, 100, and 1000 μM as indicated. *c*, Concentration–effect curves of FFA (*open circles*) and NFA (*solid circles*) for the potentiation of the peak amplitude of 10 μM ACh-induced inward current mediated by α3β4 nAChRs. Data points represent mean ± SD (error bars) of three to seven oocytes.

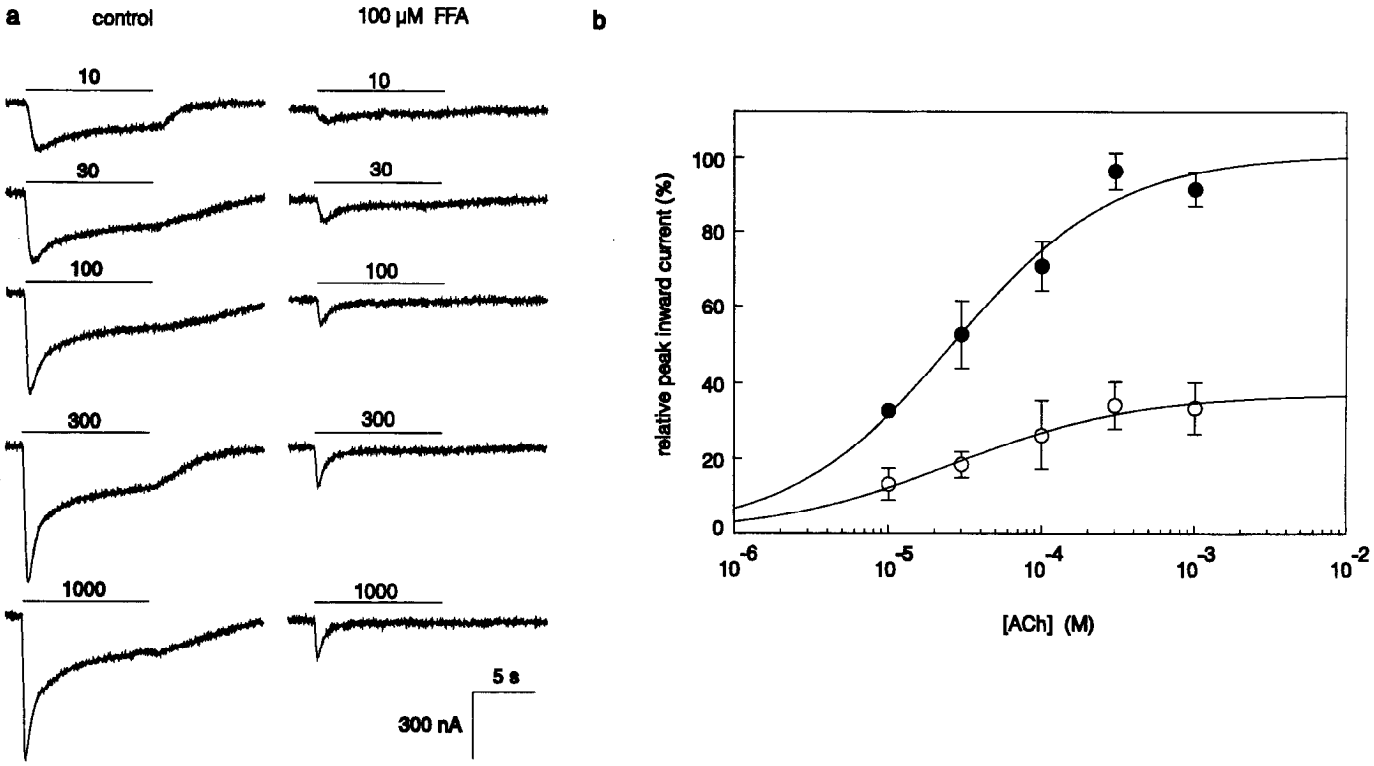

Figure 7. Effect of 100 μM FFA on the concentration–effect curve of ACh on α3β2 nAChR. *a*, Inward currents evoked by superfusion of 10, 30, 100, 300, and 1000 μM ACh (as indicated by *horizontal bars*) under control conditions and after 15 min of superfusion with 100 μM FFA. Current traces were filtered at 1 kHz. *b*, Concentration–effect curves of ACh under control conditions (*solid circles*) and in the presence of 100 μM FFA (*open circles*). Data points represent mean ± SD (errof bars) of three oocytes. For each oocyte a control concentration–effect curve was fitted with a maximum of 100 and the maximum of the concentration–effect curve in the presence of FFA was normalized to control. The lines drawn represent the mean concentration–effect curves with the mean of the parameters fitted to the data from individual oocytes. Complete reversal of the effect was obtained only after 10–15 min of washing (not shown).

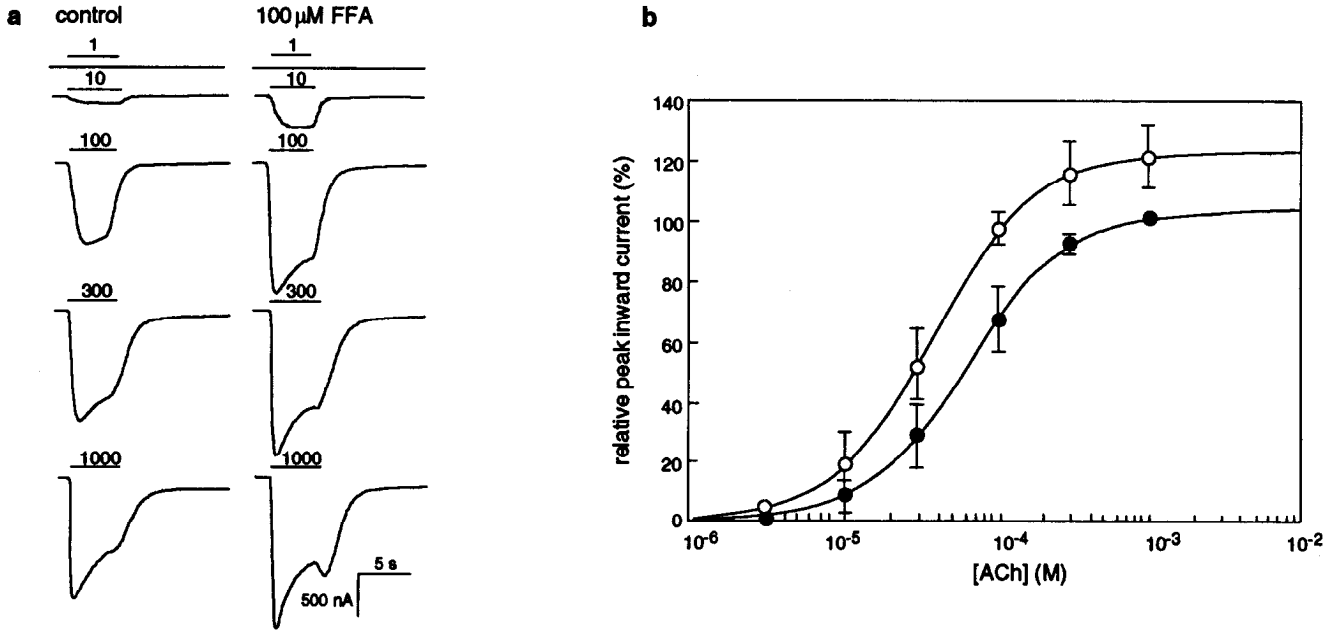

Figure 8. Effect of 100 μM FFA on the concentration–effect curve of ACh on α3β4 nAChR. *a*, Inward currents evoked by superfusion of 1, 10, 100, 300, and 1000 μM ACh (as indicated by *horizontal bars*) under control conditions and in the presence of 100 μM FFA. *b*, Concentration–effect curves of ACh under control conditions (*solid circles*) and in the continuous presence of 100 μM FFA (*open circles*). Data points represent mean ± SD (error bars) of four oocytes. For each oocyte, all peak inward current amplitudes were normalized to that of the inward current evoked by 1 mM ACh in the absence of FFA and plotted against ACh concentration. The concentration–effect curves after washout of 100 μM FFA were the same as those obtained before application of FFA (result not shown). In order to maintain the quality of voltage clamp during the large inward currents mediated by the α3β4 nAChR at high concentrations of the agonist, the membrane potential was held at −30 mV in these experiments.

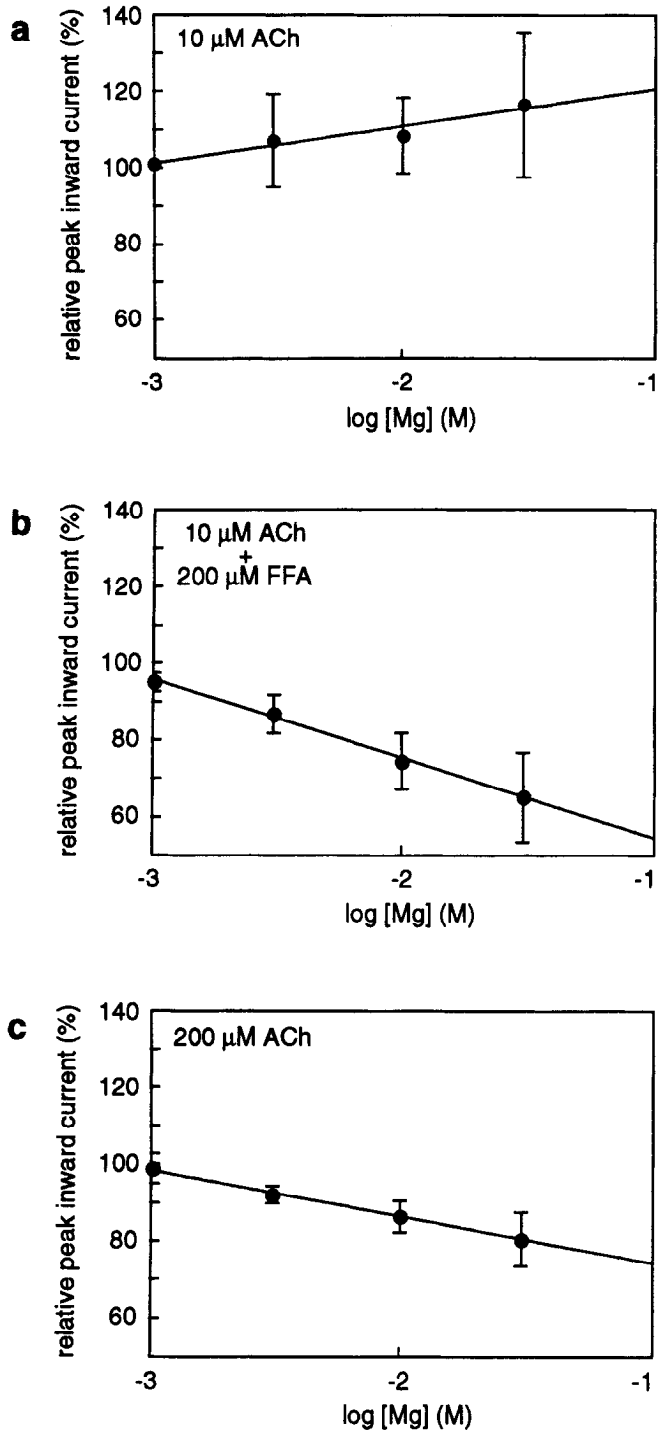

Figure 9. Relation between FFA effect and external Mg^{2+} concentration on α3β4 nAChRs. *a*, Under control conditions Mg^{2+} causes only a slight, concentration-dependent potentiation of 10 μM ACh-induced inward currents. Data points represent mean ± SD (error bars) of three oocytes. For each oocyte amplitudes were normalized to that of the 10 μM ACh-induced inward current in Cl^--free saline. Log-linear regression showed no deviation from linearity ($p = 0.81$) and the hypothesis of no regression was rejected ($p < 0.01$). *b*, In the continuous presence of 200 μM FFA Mg^{2+} blocks 10 μM ACh-induced inward currents in a concentration-dependent manner. Data points represent mean ± SD (error bars) of three oocytes. For each oocyte amplitudes were normalized to that of the 10 μM ACh-induced inward current in Cl^--free saline containing 200 μM FFA. Log-linear regression showed no deviation from linearity ($p = 0.67$) and the hypothesis of no regression was rejected ($p < 0.001$). *c*, Under control conditions 200 μM ACh-induced inward currents are also blocked by Mg^{2+} in a concentration-dependent manner. Data points represent mean ± SD (error bars) of three oocytes. For each oocyte amplitudes were normalized to 200 μM ACh-induced inward current in Cl^--free saline. Log-linear regression showed no deviation from linearity ($p = 0.68$) and the hypothesis of no regression was rejected ($p < 0.001$).

of FFA (Fig. 5) also indicates that the effects are directly on the nAChR. The β2 and β4 subunits are involved in the determination of agonist and antagonist sensitivity as well as of single channel parameters of nAChRs (see introductory section). The agonist cytisine, which is a potent agonist of β4-containing nAChR, acts as a partial agonist on β2-containing nAChR and thereby inhibits the effects of full agonists on these receptors (Luetje and Patrick, 1991; Papke and Heinemann, 1994). However, β-subunit-dependent, opposite effects as presently observed for FFA and NFA have not been reported thus far. Together with the observation, that α2β4 nAChR-mediated ion current is also potentiated by FFA (R. Zwart, unpublished result), the results suggest that the differential modulation of nAChR-mediated ion current is dependent on the β subunit.

The present results show that the compounds FFA and NFA cannot be used to separate endogenous Cl(Ca) current from neuronal nAChR-mediated current without adverse effects on the nAChRs. At the same time the results demonstrate that with the present methods the use of Cl(Ca) current blockers is not required to investigate α3β2 and α3β4 nAChRs. The lack of differences in the effects of NFA and FFA on α3β2 and α3β4 under standard Cl^- conditions and under conditions that the Cl(Ca) current cannot be activated (Figs. 2, 3) indicates that Ca^{2+} influx through the α3β2 and α3β4 nAChRs is not sufficient to activate a significant Cl(Ca) current. Our findings contrast with the previous finding that FFA and NFA block α3β4 nAChR in oocytes, suggesting that Cl(Ca) current is activated as a consequence of α3β4 nAChR stimulation in *Xenopus* oocytes (Vernino et al., 1992). Although the magnitude of Cl(Ca) currents may have been different, we have not been able to reproduce the result of the former study under identical experimental conditions.

Mechanism of potentiation and inhibition of the nAChR-mediated ion current

FFA inhibits α3β2 nAChR-mediated ion current at all ACh concentrations and causes a significant reduction of the maximum peak inward current amplitude to 38 ± 8% of the control value. The EC_{50} value and the slope factor of the concentration–effect curve of ACh remain unaffected in the presence of FFA. Conversely, FFA enhances the α3β4 nAChR-mediated ion current at all ACh concentrations and a shift of the concentration-effect curve of ACh to lower agonist concentrations is observed (Fig. 8). The change in the EC_{50} of ACh by FFA from 63 μM to 37 μM appears to be within experimental error and is likely to be overestimated. Figure 8*a* shows that FFA causes an increase of the tail current following responses evoked by high concentrations of ACh. Tail currents indicate that ion channel block has occurred during the response and is reversed on washing (Sine and Steinbach, 1984; Oortgiesen and Vijverberg, 1989). Such a blocking effect will cause underestimation of the E_{max} and EC_{50} values of the concentration–effect curve. Enhanced open channel block in the presence of FFA (Fig. 8) may account for an apparent reduction in the EC_{50} of ACh. For this reason the potentiation of α3β4 nAChR-mediated inward current as well as

←

the inhibition of α3β2 nAChR-mediated inward current by FFA are most likely due to a noncompetitive mechanism of action. Final confirmation of the noncompetitive nature of the effects of FFA would require radioligand binding experiments.

The enhancement by FFA of the α3β4 nAChR-mediated ion current at all agonist concentrations may be caused by a number of effects. The number of functional nAChR, the single nAChR channel open probability or the single nAChR channel conductance may be increased. The results of the experiments with Mg^{2+} provide a possible explanation for the mechanism involved. Mg^{2+} slightly potentiates ion current evoked by 10 μM ACh, that is, at relatively low open channel probability, and blocks responses evoked by 200 μM ACh, that is, at high open channel probability (Fig. 9). In the presence of 200 μM FFA Mg^{2+} no longer potentiates, but blocks the 10 μM ACh-induced inward current. This suggests that, like an increase of the agonist concentration, FFA increases the single channel open probability and thereby facilitates divalent cation block. An increase in the number of functional nAChR in the presence of FFA is a less likely explanation for the potentiating effects. In that case, Mg^{2+} should block the ion current to the same extent in the absence and in the presence of FFA. The various potentiations of neurotransmitter receptor-operated ion current reported thus far are all caused by an increase in single channel open probability. The potentiating effects of Ca^{2+} on neuronal nAChRs (Vernino, 1992; Mulle et al., 1992b), glycine on NMDA receptors (Johnson and Ascher, 1987), and benzodiazepines on $GABA_A$ receptors (Sieghart, 1992) are due to an increase in opening frequency of the channels and the potentiating effect of barbiturates on $GABA_A$-receptors (Sieghart, 1992) is due to an increase in mean channel open time. In order to discriminate between the different possible mechanisms of potentiation by FFA and of potentiation and block by Mg^{2+} single channel studies are required.

It is concluded that α3β4 and α3β2 nAChRs are oppositely modulated by FFA and NFA through a direct β subunit-dependent effect, resulting in potentiation and inhibition of agonist-induced ion currents. The results raise the important question whether endogenous ligands exist, which by non-competitive modulation of neuronal nAChRs differentially affect the functioning of cholinergic neurons *in vivo*.

References

Anand R, Conroy WG, Schoepfer R, Whiting P, Lindstrom J (1991) Neuronal nicotinic acetylcholine receptors expressed in *Xenopus* oocytes have a pentameric quaternary structure. J Biol Chem 266: 11192–11198.

Barish ME (1983) A transient calcium-dependent chloride current in the immature *Xenopus* oocyte. J Physiol (Lond) 342:309–325.

Bertrand D, Cooper E, Valera S, Rungger D, Ballivet M (1991) Electrophysiology of neuronal nicotinic acetylcholine receptors expressed in *Xenopus* oocytes following nuclear injection of genes or cDNAs. Methods Neurosci 4:174–193.

Bertrand D, Galzi JL, Devillers-Thiéry A, Bertrand S, Changeux JP (1993) Mutations at two distinct sites within the channel domain M2 alter calcium permeability of neuronal α7 nicotinic receptor. Proc Natl Acad Sci USA 90:6971–6975.

Boulter J, Connolly J, Deneris E, Goldman D, Martin G, Treco D, Heinemann S, Patrick J (1986) Isolation of a cDNA clone coding for a possible neural nicotinic acetylcholine receptor α-subunit. Nature 319:368–374.

Boulter J, O'Shea-Greenfield A, Duvoisin R, Connolly J, Wada E, Jensen A, Ballivet M, Deneris E, Heinemann S, Patrick J (1990) α3, α5 and β4: three members of the rat neuronal nicotinic acetylcholine receptor-related gene family form a gene cluster. J Biol Chem 265: 4472–4482.

Cachelin AB, Jaggi R (1991) β subunits determine the time course of desensitization in rat α3 neuronal nicotinic acetylcholine receptors. Pfluegers Arch 419:579–582.

Cooper E, Couturier S, Ballivet M (1991) Pentameric structure and subunit stoichiometry of a neuronal nicotinic acetylcholine receptor. Nature 350:235–238.

Couturier S, Bertrand D, Matter JM, Hernandez MC, Bertrand S, Millar N, Valera S, Barkas T, Ballivet M (1990) A neuronal nicotinic acetylcholine receptor subunit (α7) is developmentally regulated and forms a homo-oligomeric channel blocked by α-BTX. Neuron 5:847–856.

Deneris ES, Connolly J, Boulter J, Wada E, Wada K, Swanson LW, Patrick J, Heinemann S (1988a) Primary structure and expression of beta-2: a novel subunit of neuronal nicotinic acetylcholine receptors. Neuron 1:45–54.

Deneris ES, Boulter J, Swanson L, Patrick J, Heinemann S (1988b) β-3, a new member of the nicotinic acetylcholine receptor gene family is expressed in the brain. J Biol Chem 264:6268–6272.

Deneris ES, Connolly J, Rogers SW, Duvoisin R (1991) Pharmacological and functional diversity of neuronal nicotinic acetylcholine receptors. Trends Pharmacol Sci 12:34–40.

Duvoisin RM, Deneris ES, Boulter J, Patrick J, Heinemann S (1989) The functional diversity of the neuronal nicotinic acetylcholine receptors is increased by a novel subunit: β4. Neuron 3:487–496.

Fieber LA, Adams DJ (1991) Acetylcholine-evoked currents in cultured neurones dissociated from rat parasympathetic cardiac ganglia. J Physiol (Lond) 434:215–237.

Galzi JL, Devillers-Thiéry A, Hussy N, Bertrand S, Changeux JP, Bertrand D (1992) Mutations in the channel domain of a neuronal nicotinic receptor convert ion selectivity from cationic to anionic. Nature 359:500–505.

Goldman D, Deneris ES, Luyten W, Kochhar A, Patrick J, Heinemann S (1987) Members of a nicotinic acetylcholine receptor gene family are expressed in different regions of the mammalian central nervous system. Cell 48:965–973.

Johnson JW, Ascher P (1987) Glycine potentiates the NMDA response of mouse central neurones. Nature 325:529–531.

Lamar E, Miller K, Wadiche J, Patrick J (1990) Amplification of genomic sequences identifies a new gene, alpha6, in the nicotinic acetylcholine receptor gene family. Soc Neurosci Abstr 16:681.

Leonard JP, Kelso SR (1990) Apparent desensitization of NMDA responses in *Xenopus* oocytes involves calcium-dependent chloride current. Neuron 4:53–60.

Lerma, J, Martín del Río R (1992) Chloride transport blockers prevent *N*-methyl-D-aspartate receptor-channel complex activation. Mol Pharmacol 41:217–222.

Luetje CW, Patrick J (1991) Both alpha- and beta-subunits contribute to the agonist sensitivity of neuronal nicotinic acetylcholine receptors. J Neurosci 11:837–845.

Luetje CW, Patrick J, Séguéla P (1990) Nicotine receptors in the mammalian brain. FASEB J 4:2753–2760.

Marquardt DW (1963) An algorithm for least-squares estimation of nonlinear parameters. J Soc Indust Appl Math 11:431–441.

Miledi R, Parker I (1984) Chloride current induced by injection of calcium into *Xenopus* oocytes. J Physiol (Lond) 357:173–183.

Mulle C, Choquet D, Korn H, Changeux JP (1992a) Calcium influx through nicotinic receptor in rat central neurons: its relevance to cellular regulation. Neuron 8:1–9.

Mulle C, Lena C, Changeux JP (1992b) Potentiation of nicotinic receptor response by external calcium in rat central neurons. Neuron 8:937–945.

Oortgiesen M, Vijverberg HPM (1989) Properties of neuronal type acetylcholine receptors in voltage clamped mouse neuroblastoma cells. Neuroscience 31:169–179.

Papke RL, Heinemann SF (1991) The role of the β4 subunit in determining the kinetic properties of rat neuronal nicotinic acetylcholine α3-receptor. J Physiol (Lond) 440:95–112.

Papke RL, Heinemann SF (1994) Partial agonist properties of cytisine on neuronal nicotinic receptors containing the β2 subunit. Mol Pharmacol 45:142–149.

Papke RL, Duvoisin RM, Heinemann SF (1993) The amino terminal half of the nicotinic β-subunit extracellular domain regulates the kinetics of inhibition by neuronal bungarotoxin. Proc R Soc Lond B 252:141–148.

Sands SB, Barish ME (1991) Calcium permeability of neuronal nico-

tinic acetylcholine receptor channels in PC12 cells. Brain Res 560: 38–42.

Sands SB, Costa ACS, Patrick JW (1993) Barium permeability of neuronal nicotinic receptor α7 expressed in *Xenopus* oocytes. Biophys J 65:2614–2621.

Schoepfer R, Conroy W, Whiting P, Gore M, Lindstrom J (1990) Brain α-bungarotoxin binding protein cDNAs and mABs reveal subtypes of this branch of the ligand-gated ion channel gene superfamily. Neuron 5:35–48.

Séguéla P, Wadiche J, Dineley-Miller K, Dani JA, Patrick JW (1993) Molecular cloning, functional expression and distribution of rat brain α7: a nicotinic cationic channel highly permeable to calcium. J Neurosci 13:596–604.

Sieghart W (1992) $GABA_A$ receptors: ligand-gated Cl^- ion channels modulated by multiple drug-binding sites. Trends Pharmacol Sci 13: 446–450.

Sine SM, Steinbach JH (1984) Agonists block currents through acetylcholine receptor channels. Biophys J 46:277–284.

Stafford GA, Oswald RE, Weiland GA (1994) The beta subunit of neuronal nicotinic acetylcholine receptors is a determinant of the affinity for substance P inhibition. Mol Pharmacol 45:758–762.

Trouslard J, Marsh SJ, Brown DA (1993) Calcium entry through nicotinic receptor channels and calcium channels in cultured rat superior cervical ganglion cells. J Physiol (Lond) 468:53–71.

Vernallis AB, Conroy WG, Berg DK (1993) Neurons assemble acetylcholine receptors with as many as three kinds of subunits while maintaining subunit segregation among receptor subtypes. Neuron 10:451–464.

Vernino S, Amador M, Luetje CW, Patrick J, Dani JA (1992) Calcium modulation and high calcium permeability of neuronal nicotinic acetylcholine receptors. Neuron 8:127–134.

Wada K, Ballivet M, Boulter J, Connolly J, Wada E, Deneris ES, Swanson LW, Heinemann S, Patrick J (1988) Functional expression of a new pharmacological subtype of brain nicotinic acetylcholine receptor. Science 240:330–334.

White MM, Aylwin M (1990) Niflumic and flufenamic acids are potent reversible blockers of calcium-activated chloride channels in *Xenopus* oocytes. Mol Pharmacol 37:720–724.

Woodward RM, Polenzani L, Miledi R (1994) Effects of fenamates and other nonsteroidal anti-inflammatory drugs on rat brain $GABA_A$ receptors expressed in *Xenopus* oocytes. J Pharmacol Exp Ther 268: 806–817.

Zhou Z, Neher E (1993) Calcium permeability of nicotinic acetylcholine receptor channels in bovine adrenal chromaffin cells. Pfluegers Arch 425:511–517.